Fast Noncontinuous Path Phase-Unwrapping Algorithm Based on Gradients and Mask

Carlos Díaz and Leopoldo Altamirano Robles

National Institute of Astrophysics, Optics and Electronics, Luis Enrique Erro # 1, Santa Maria Tonantzintla, Puebla, 72840, Mexico
{cdiaz,robles}@inaoep.mx

Abstract. Various algorithms based on unwrapping first the most-reliable pixels have been proposed. These were restricted to continuous path and were subject to troubles on defining an initial pixel. The technique proposed uses a reliability function that helps us to define starting points, it does not follow a continuous path to perform the unwrapping operation, and it uses a mask to pick out invalid pixels. The technique is explained with all the specifics and exemplify with some examples.

1 Introduction

Optical techniques such as 3D profilometry, photoelasticity, and interferometry have the advantage of being noncontact, fast, and capable of providing whole-field information. They have already been developed for measuring a wide range of physical parameters such as stress, vibration, displacement, and surface profile. In all these techniques, the measured parameters are modulated in the form of a 2D fringe pattern. Demodulation by the use of fringe pattern processing is thus an essential and important procedure.

First a wrapped phase map whose principal values range from $-\pi$ to π is calculated from the fringe pattern. Phase unwrapping is then carried out to restore the unknown multiple of 2π to each pixel. When the recorded images satisfy the Nyquist criteria, the phase unwrapping process is straightforward. If the phase difference calculated for two adjacent points is equal to 2π, then 2π or multiples of 2π must be added to or subtracted from the calculated value of the second pixel. The entire phase map is obtained by working outward from the starting location.

The diagram can explain the whole idea. Figure 1 shows the phase values calculated by arctangent at each pixel. Figure 2 shows the true phase values that are found by adding the correct number of 2π's to each of these values. The above process only shows how to do 1D unwrapping. However, it is very easy to extend the 1D process to unwrap a 2D map.

When phase wrap is getting by phase shifting interferometry there are additional information as data modulation that can aid in phase unwrap process.

The paper includes four sections: section 1 provides an overview of some existing phase-unwrapping algorithms, section 2 presents our proposal, section 3 gives experimental results of our algorithm, and finally, section 4 are conclusions.

A. Sanfeliu et al. (Eds.): CIARP 2004, LNCS 3287, pp. 116–123, 2004.

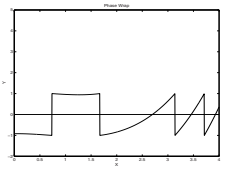

Fig. 1. 1D phase wrap distribution.

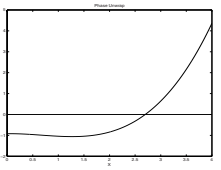

Fig. 2. 1D phase unwrap distribution.

2 Existing Phase-Unwrapping Algorithms

The phase unwrapping process is like a simple connect-thedots game. However, things can be very complicated because of all kinds of error sources, especially when an automated phase unwrapping process is required. The error sources that arise most frequently in a fringe pattern are as follows:

1. Background noise or electronic noise produced during data acquisition.
2. Low data modulation points due to low surface reflectivity.
3. Abrupt phase changes due to surface discontinuities or shadows.
4. Violation of the sampling theorem (less than two sampling points per fringe). This error can cause the images to be totally unusable.

Most phase unwrapping algorithms can handle (1) and (2). (4) can be avoided by changing system setup. For error source (3), one needs to have a priori knowledge of the object or to use special techniques. Otherwise (3) will result in path-dependent phase unwrapping which is unacceptable.

A major goal of fringe analysis is to automate the phase unwrapping process. Automatic techniques are essential if systems are in a unsupervised way or high speed processing is in demand. Extensive research has been done in the development of phase unwrapping algorithms. However, a general approach to the problem of automated phase unwrapping in fringe analysis has been lacking. The following sections briefly review some of the representative phase unwrapping techniques.

2.1 Phase Fringe Scanning Method

Greivenkamp proposed this method in [7]. A horizontal line of the phase image is unwrapped first. Then starting at each point on this line, the whole phase map is unwrapped vertically. This is the most straightforward method of phase unwrapping and therefore is the fastest one among all phase unwrapping techniques. Unfortunately, this method can not handle phase images of objects with areas of low surface reflectivity.

2.2 Phase Unwrapping by Sections

Arevallilo and Burton developed this algorithm [1, 3]. An image can be subdivided into four sections. If a section is larger than 2×2 pixels, this section is

further subdivided into four sections. It is easy to unwrap a 2×2 area (4 pixels) and two areas can be connected by checking their common edge. After sub-areas have been unwrapped, they are joined together. Points on the edge are traced to judge if a shift should be made, up by 2π, down by 2π, or no shift according to certain weighted criterion. This method tends to provide global unwrapping optima but has the complexity to deal with error source areas. The weighted criterion for connecting sections is also difficult to be used as a general criterion.

2.3 Phase Unwrapping by Using Gradient

This method was proposed by Huntley [8] in an attempt to solve the problem of surface discontinuity. Since a large phase difference between any two adjacent pixels increments the possibility of a discontinuous phase change, this algorithm always tries to choose the direction of the smallest gradient to unwrap phase. The phase at each pixel is compared with its 8 neighboring pixels. The direction in which the phase difference is the smallest is taken to unwrap the phase.

The drawback of this algorithm is that invalid pixels are phase unwrapped eventually, which introduce phase unwrapping errors. One solution to this problem is to set a threshold phase difference to reject invalid pixels due to noise or phase discontinuity. The threshold has to be flexible in order to adapt to different circumstances, which makes automatic phase unwrapping difficult. Using the first phase difference may result in misjudgment in choosing the right unwrapping direction. In [2, 4] is proposed the second order difference method which is used to improve the performance. Phase unwrapping based on least gradient does provide the most logic way for phase unwrapping. However, the method may not be able to unwrap all the pixels of interest automatically and to handle zones of high curvature of phase map.

3 Our Phase Unwrapping Algorithm Proposal

The phase unwrapping by using gradients approach provides the most logic way for phase unwrapping. The algorithm proposed in this research takes advantage of this approach and uses additional information obtained in data modulation to eliminate errors in the phase image. First of all, part of the fringe images may be saturated due to specular reflection. These pixels have to be excluded from the phase unwrapping process because they do not provide correct phase information. Also, the object may not fill the entire image and it may also have holes on its surface. This often results in a phase image with substantial background noise. All the pixels representing the background should also be excluded from the phase unwrapping process. These saturated pixels and background pixels are identified by calculating the data modulation at each pixel. Assigning a threshold value to the data modulation, a generated mask defines the areas of valid and invalid pixels. Phase unwrapping is done only at valid pixels.

The whole procedure can be summarized as the following steps:

1. *Generate Mask.* To generate a mask image M based on the data modulation calculation. This mask image indicates whether a pixel is valid or not. Only valid pixels are processed in the automatic unwrapping procedure. In figure 3, the black area represents an area of invalid pixels of the phase wrap distribution shown in figure 8.

Fig. 3. Binary mask, black area represents invalid pixels.

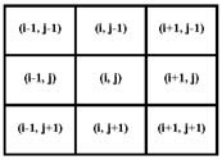

Fig. 4. Calculation of the second derivative in an image.

2. *Calculate Reliability Values.* In this step, we based upon the gradients. Those points with the lowest module 2π gradients with respect to their neighbors are determined to be the best points, therefore, these points are processed first.
Second derivative would provide a measurement for the degree of concavity/convexity of the phase function. By use of second derivative a better detection of possible inconsistencies in the phase map is provided. The calculation of second derivative for pixels in an image can be explained with the aid of figure 4. To calculate the second difference for a pixel in an image, the values of its orthogonal and diagonal neighbors in a 3×3 window are required. The pixels $(i, j-1)$, $(i, j+1)$, $(i-1, j)$, and $(i+1, j)$ that are neighbors to the (i, j) pixels are called orthogonal neighboring pixels. Whereas $(i-1, j-1)$, $(i+1, j-1)$, $(i-1, j+1)$, and $(i+1, j+1)$ pixels are called diagonal neighboring pixels. The second difference D of an (i, j) pixel can be calculated by the equation:

$$D(i,j) = \sqrt{H^2(i,j) + V^2(i,j) + D_1^2(i,j) + D_2^2(i,j)}\,. \tag{1}$$

$$\begin{aligned}
H(i,j) &= \gamma[\phi(i-1,j) - \phi(i,j)] - \gamma[\phi(i,j) - \phi(i+1,j)]\,,\\
V(i,j) &= \gamma[\phi(i,j-1) - \phi(i,j)] - \gamma[\phi(i,j) - \phi(i,j+1)]\,,\\
D_1(i,j) &= \gamma[\phi(i-1,j-1) - \phi(i,j)] - \gamma[\phi(i,j) - \phi(i+1,j+1)]\,,\\
D_2(i,j) &= \gamma[\phi(i-1,j+1) - \phi(i,j)] - \gamma[\phi(i,j) - \phi(i+1,j-1)]\,.
\end{aligned}$$

where $\gamma[(.)]$ is a simple unwrapping operation to remove any 2π steps between two consecutive pixels. The second derivative should be calculated for all valid pixels in M. The reliability R of a pixel is defined as:

$$R(i,j) = \frac{1}{D(i,j)}\,. \tag{2}$$

Consequently, pixels are more reliable if their second derivatives are lower.

3. *Edge Computation.* For this research an edge is considered an intersection of two pixels that are connected horizontally or vertically. Any pixel with its left hand side, right hand side, upper, or lower neighboring pixel can construct an edge. Every two orthogonal neighboring pixels can produce an edge.
   We only compute edges of valid pixels in M. An unwrapping path cannot be defined relative to the reliability of the pixels. Instead, it is defined by looking at the value of the reliability of the edges. We define edge reliability as the summation of the reliabilities of the two pixels that the edge connects:

$$R_{e_{k,l}} = R_k + R_l \, . \tag{3}$$

   where $R_{e_{k,l}}$ is the edge's reliability defined by k and l pixels.
4. *Initialize Groups.* Initially all valid pixels are considered not belonging to any group. Not valid pixels are considered belonging to group 0, that it won't be considered in automatic phase unwrap process.
5. *Unwrapping Path.* In unwrapping path those valid edges with higher reliability are unwrapped first. The edges are stored in an array and sorted by value of reliability. The edges with a higher reliability are resolved first. When the process is performed, pixels form groups of pixels. When is analyzed an edge in the unwrapping process, three cases are possible:
   (a) Both pixels have not been unwrapped before. The pixels are unwrapped with respect to each other and gathered into a single group of unwrapped pixels.
   (b) One of the pixels has been processed before, P_1 but the other has not, P_2. P_2 is unwrapped with respect to P_1 and added to the P_1's group.
   (c) Both pixels have been processed before. If they do not belong to the same group, the two groups need to be unwrapped with respect to each other. The smallest group is unwrapped with respect to the largest group.

If the wrapped phase map is composed of disconnected valid parts, the above steps finish all parts without depending on where the starting point is located. Certain relationships among these separate parts have to be predetermined in order to connect the whole surface.

4 Simulated and Experimental Results

The proposed algorithm has been tested using simulated and experimental images. All images depicting phase distribution are scaled between black and white for display.

Simulated Results. Figure 5(a) shows a simulated wrapped phase distribution with no noise and no physical discontinuities present. This image has been used to test the proposed algorithm under ideal conditions. Figure 5(b) shows the simulated unwrapped phase.

Figure 5(c) shows a simulated wrapped phase distribution in which there is no noise in the body of the phase, but there is a small central area that contains

only random noise. The purpose of this data set is to test the unwrapper's ability to isolate this noise and to prevent it from corrupting the unwrapping of the good data. Figure 5(d) shows the simulated unwrapped phase map.

We make a comparison between unwrapped phase simulated depicted in figures 5(b) and 5(d), and unwrapped phase obtained by algorithms show in figures 6 and 7, and we obtain a consistent in pixels values of 93%, see table 2. We compute percent of phase consistency by subtracting the phase unwrap obtained by any method from the reference phase unwrap distribution.

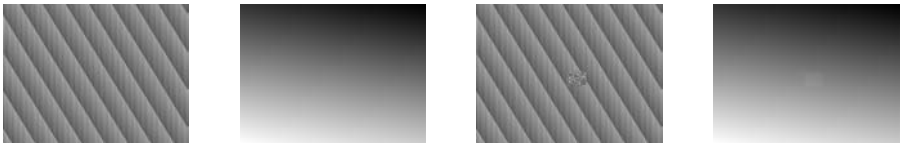

(a) Wrapped phase without noise. (b) Unwrapped phase without noise. (c) Wrapped phase with a noise area. (d) Unwrapped phase distribution with a noise area.

Fig. 5. Simulated phase distribution.

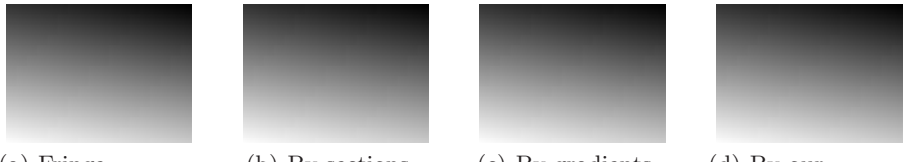

(a) Fringe scanning. (b) By sections. (c) By gradients. (d) By our method.

Fig. 6. Phase unwrap results of phase wrap show in figure 5(a).

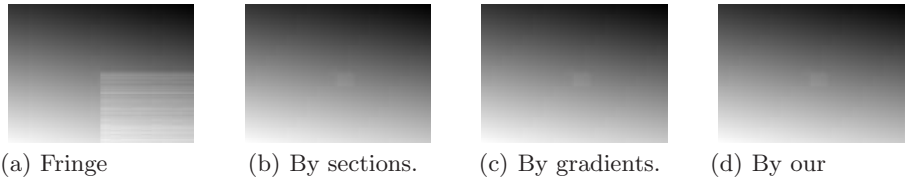

(a) Fringe scanning. (b) By sections. (c) By gradients. (d) By our method.

Fig. 7. Phase unwrap results of phase wrap show in figure 5(c).

Experimental Results. Figure 8 shows a wrapped phase map resulting from the analysis of a real fringe pattern. The wrapped phase map contains corrupted areas that result from a shadow of the projected fringes. The wrapped phase map has been unwrapped using the proposed algorithm. The unwrapped phase

Table 1. Percent of phase unwrap distribution consistent between simulated and obtained phase unwrap without noise (see table 2).

Method	Percent of consistency	Time (in seconds)
Fringe scanning	99%	0.32
Sections	96%	1.85
Gradients only	95%	1.91
Our proposal	96%	1.71

Table 2. Percent of phase unwrap distribution consistent between simulated and obtained phase unwrap with noise.

Method	Percent of consistency	Time (in seconds)
Fringe scanning	78%	0.35
Sections	89%	2.30
Gradients only	91%	2.11
Our proposal	93%	1.82

map is shown in figure 9, which indicates that the algorithm was capable of unwrapping the unreliable regions last to prevent error propagation. The algorithm copes well with these problems and successfully unwraps the image. A 3D representation of the unwrapped phase map is shown in figure 10. The dynamic range of the unwrapped phase map can be more larger than the dynamic range of the wrapped phase map. The displaying of the unwrapped phase map by scaling it between black and white is not always indicative of the unwrapping process being performed correctly. Therefore following Ghiglia and Romero's method [6], we rewrapped the unwrapped phase map to permit a direct comparison with the wrapped image. This rewrapping is visually convincing that the unwrapping is qualitatively correct. Figure 11 shows the rewrapped phase map of the unwrapped phase map shown in figure 9. Figures 8 and 11 show a good agreement between the wrapped and the rewrapped phase maps, which demonstrates that the proposed algorithm unwrapped the wrapped phase map successfully.

Fig. 8. Wrapped phase distribution.

Fig. 9. Unwrapped phase distribution.

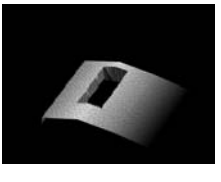

Fig. 10. 3D representation of the resulting phase.

Fig. 11. Rewrapped phase map.

The execution time of the proposed algorithm varies from image to image and depends on the particular phase distribution being analyzed. The tested

images are 640 × 480 pixels in size. The proposed algorithm has been executed on a PC system. The PC contains a Pentium 4 processor that runs at 2.0 GHz clock speed. The memory on this PC is 256 MB RAM. The execution time is in the order of two seconds on average. The execution time to unwrap the image shown in figure 8 was 1.8 seconds.

5 Conclusions

A fast, reliable 2D unwrapper has been proposed, described, and tested. The algorithm that follows a noncontinuous path and, is based on unwrapping points with higher reliability values, it produces consistent results when discontinuities or noisy areas are presented.

The above algorithm works closely with the masking technique based on data modulation to provide a fast and reliable phase unwrapping method. Compared to the previously developed algorithms reviewed in the previous section, this new algorithm is simple and fast yet produces comparable good results.

References

1. M. Arevallilo Herraéz, D. R. Burton, and D. B. Clegg, "Robust, Simple, and Fast Algorithm for Phase Unwrapping", Applied Optics, 1996, Vol. 35, 5847-5852.
2. M. Arevallilo Herraéz, D. R. Burton, M. J. Lalor, and M. A. Gdeisat, "Fast Two-Dimensional Automatic Phase Unwrapping Algorithm Based on Sorting by Reliability Following a Noncontinuous Path", Applied Optics, 2002, Vol. 41, No. 35, 7437-7444.
3. M. Arevallilo Herraéz, M. A. Gdeisat, D. R. Burton, and M. J. Lalor, "Robust, Fast, and Effective Two-Dimensional Automatic Phase Unwrapping Algorithm Based on Image Decomposition", Applied Optics, 2002, 41, 35, 7445-7455.
4. R. Cusack, J. M. Huntley, and H. T. Goldrein, "Improved Noise-Immune Phase-Unwrapping Algorithm", in Applied Optics, Vol. 34, No. 5, 781-789, 1995.
5. D. C. Ghiglia, G. A. Masting, and L. A. Romero, "Cellular-Automation Method for Phase Unwrapping", in Journal of Optical Society of America, Vol. 4, No. 5. 267-280, 1987.
6. D. C. Ghiglia, and L. A. Romero, "Robust Two-Dimensional Weighted Phase Unwrapping that Uses Fast Transforms and Iterative Methods", in Journal of Optical Society of America, Vol. 11, No. 1. 107-117, 1994.
7. J. E. Greivenkamp and J. H. Bruning, "Phase Shifting Interferometers", in Optical Shop Testing, D. Malacara, 2nd Ed. 501-598, Wiley, New York, 1992.
8. J. M. Huntley and H. O. Saldner, "Error Reduction Methods for Shape Measurement by Temporal Phase Unwrapping", in Journal of Optical Society of America, Vol. 14, No. 2. 3188-3196, 1997.